CONFERENCE PROCEEDINGS

Surface Mixing as Method for Minimizing Leakage Risk in CO2 Sequestration

Surface Mixing as Method for Minimizing Risk in CO2 Sequestration

McMillan Burton, Steven L. Bryant

SIXTH ANNUAL CONFERENCE ON CARBON CAPTURE AND SEQUESTRATION - DOE/NETL
May 7 - 10, 2007

Author Information

McMillan Burton
Research Assistant
University of Texas at Austin
Dept of Petroleum and Geosystems Engr.
1 University Station C0300
Austin, TX 78712-0228
burton_mac@hotmail.com
512.784.9750

Steven Bryant
Associate Professor
University of Texas at Austin
Dept of Petroleum and Geosystems Engr.
1 University Station C0300
Austin, TX 78712-0228
steven_bryant@mail.utexas.edu
512.471.3250

Abstract

The economic feasibilities of geologic CO_2 sequestration and stakeholder acceptance of the technology must account for the risk of leakage from the target formation. The standard approach to geologic sequestration assumes that CO_2 will be injected as a bulk phase. In this approach, the primary driver for leakage is the buoyancy of CO_2 under typical deep conditions (depths > 800 m). An alternative approach is to dissolve the CO_2 into brine at the surface, then inject the saturated brine into deep subsurface formations. The CO_2-laden brine is slightly denser than brine containing no CO_2, so ensuring the complete dissolution of all CO_2 into brine at the surface prior to injection will eliminate the risk of buoyancy-driven leakage.

In this paper, we examine the feasibility of dissolution of CO_2 in surface facilities and injection of the saturated brine. We compute the incremental cost of the additional processes and facilities relative to injecting bulk phase CO_2. We also estimate the power requirements to determine the operating costs. The incremental capital and operating costs can be regarded as the price of this form of risk reduction. A full cost-benefit assessment requires an estimate of the cost of long-term monitoring for leakage. Such an estimate is beyond the scope of this study.

Introduction

A typical case of interest is the CO_2 emission from a 1000MW coal-fired power plant which amounts to 8Mt/year (Benson, 2006) with realistic capture of 90% of the CO_2 (Fisher, Beitler, Rueter, Searcy, Rochelle, & Jassim, 2005). The mass, mole, and volumetric flow rates of the captured stream are shown in Table 1. For this plant emission, we will compare the injection of CO_2 saturated brine against a base case of bulk carbon dioxide into the same aquifer. In an aquifer, the injection can occur at a bottomhole pressure typically between 100 psi to 1000 psi above the reservoir pressure for both strategies. The aquifer of interest is at depth of 5,800ft, pressure of 2600psia, and temperature of 141°F. We assume a constant injectivity for each well of 35,000 bbl/d of brine (5,600 m^3/d) or 125 mmscf/d of CO_2 (7,000 tonne/d).

Methods

To determine the volume of brine required to dissolve CO_2 in surface facilities, we used two equations of state tuned to different sets of measurements. The cost of obtaining the brine was neglected; the presumed source is local surface water (lake or sea) or a large wastewater stream from some other facility. (The feasibility of extracting the source brine from a deep aquifer will be examined in future work.) To determine the cost of dissolving CO_2, we estimated the power requirements for the compression of CO_2 and the compression of brine with appropriate models. The capital costs of the compression

equipment, mixing vessel, and injection wells are also estimated. The assumption of a fixed injection rate for each well makes the estimates independent of the properties of the aquifer. A description of the saturated brine injection strategies is found in Figure 1 and the CO_2 bulk phase injection strategy is found in Figure 2.

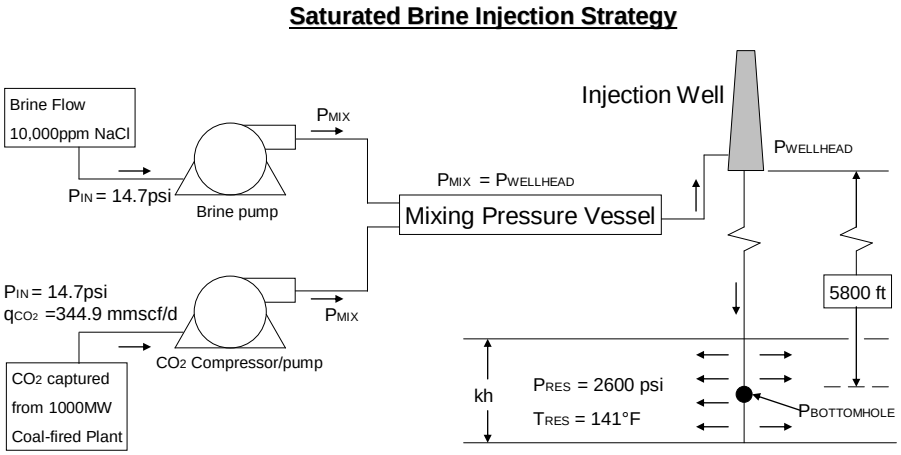

Figure 1—Schematic of the saturated brine injection strategy includes pumps for the brine and compressors/pumps for the captured CO_2 stream. The two fluids are then mixed until the CO_2 dissolves, and the saturated brine is then sent to the injection wells for disposal. The injection wells are assumed to be capable of handling 35,000 B/D of saturated brine.

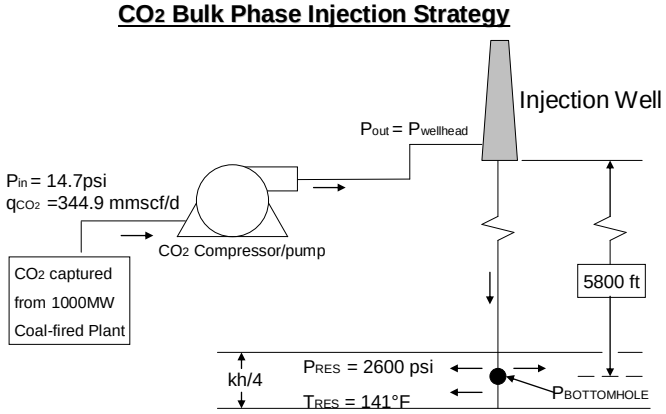

Figure 2—Schematic of the CO2 bulk phase injection (base case) strategy includes only the captured stream which is compressed to an appropriate pressure prior to injection. Injection wells are assumed to be capable of disposing 125 MMSCF/D of CO_2.

Solubility Model

We modeled the solubility of CO_2 in brine with the Peng-Robinson equation of state using the program PVTSim by Calsep Inc. (http://www.calsep.com/) and using the Duan equation of state fitted by Hangx (2005). The solubility is a function of pressure, temperature, and salinity (sodium chloride, NaCl). We fixed the temperature of the CO_2/brine mixing vessel at 68°F (20°C), but we varied the pressure and salinity to observe the solubility dependency. With the solubility expressed as mole fraction and the rate of CO_2 from the power plant (shown in Table 1), the required volumetric flow rate of brine can be determined from the equation given in Table 2 and the properties in Table 3.

Figure 3, Peng-Robinson equation of state, and Figure 4, Duan equation of state, are plots of the solubility of CO_2 and the corresponding flow rate of brine saturated with CO_2 for salinities of 0ppm and 10,000ppm.

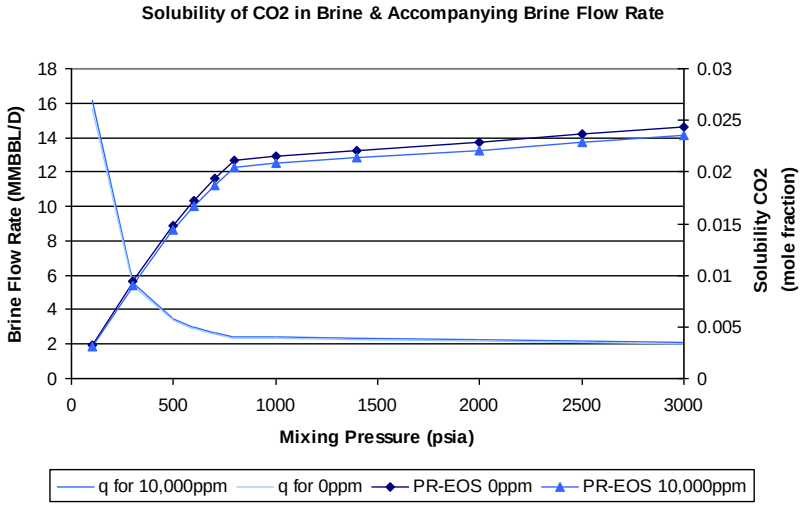

Figure 3—The solubility of CO_2 in brine at 68°F is shown for pressure of 100psia to 3000psia and salinities of 0ppm and 10,000ppm (NaCl) using the Peng-Robinson EOS with the scale for solubility on the right hand side. For a 1000MW coal-fired power plant, the flow rate of brine needed to dissolve all the captured CO_2 ranges from 2 mmbbl/d to 16 mmbbl/d, with the smaller value applicable for mixing tank pressures greater than about 1000 psia.

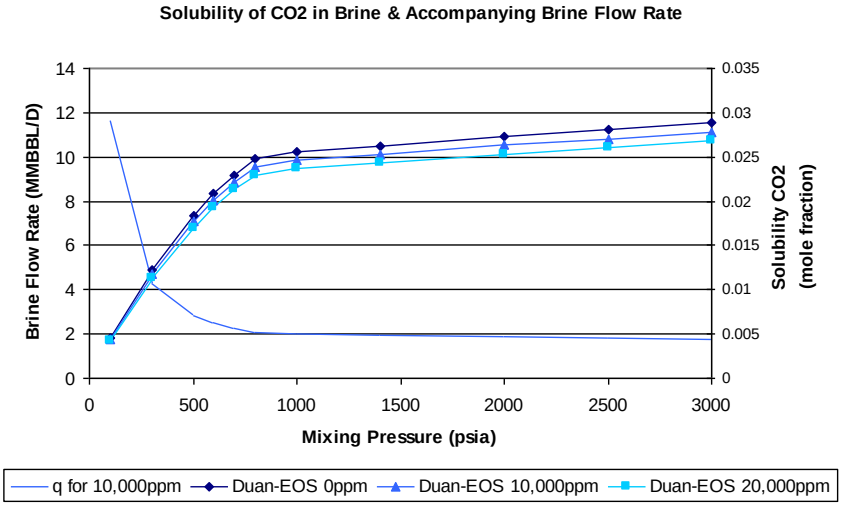

Figure 4—The solubility of CO2 in brine at 68°F is shown for pressure of 100psia to 3000psia and salinities of 0ppm, 10,000ppm, and 20,000ppm (NaCl) using the Duan EOS (Hangx, 2005). The trends are the same as the Peng-Robinson EOS, Fig. 3, but solubility is 20-30% greater. We are confident (95%) that the error in the Duan EOS is less than 10% at 0 ppm from the source data from Weibe & Gaddy (1940).

Both equations of state predict similar trends but differ in magnitude. Hangx source (Weibe & Gaddy, 1940) suggest that Duan's EOS error from the data is less than 10% (with 95% confidence) so we chose the Duan EOS for the remainder of the calculations.

Wellbore Model

The wellhead pressure required to inject into this typical aquifer depends on the properties of the formation and the properties of the injected fluid. Before we proceed to the wellbore model, we quantified the limiting properties for the formation used a simple

reservoir model. To limit the range of possibilities, we selected typical injection wells that could handle 35,000 bbl/d of brine or 125 mmscf/d of CO_2. We also limited the bottomhole pressure to between 100 and 1000 psi above the reservoir pressure (which will be termed in the subsequent figures as bottomhole pressure difference). Because saturated brine injection is the limiting case, we estimate the minimum permeability-height product (kh) for our reservoir is 2.5×10^5 md-ft (see Table 2 for explanation). Given that an aquifer with this minimum requirement can be obtained, we assume that the injections occur at the same bottomhole pressure difference only for the sake of easy comparison.

With that in mind, the wellbore model is applicable to either strategy. Based on the mechanical energy balance, it includes the contribution of gravity and the loss due to friction in the pressure profile along the length of the well. The discretization and rearrangement of the mechanical energy balance are found in Table 3. We use the wellbore model to determine the pressure at the wellhead from the pressure at the bottom of the well. The bottomhole pressure is treated as an independent variable. We chose values in the range of 100 psia to 1000 psia above the reservoir pressure. The wellhead pressure can be plotted as a function of the bottomhole pressure difference (see Figure 5). The wellhead pressure to inject CO_2 bulk phase is typically 500-900psi more than for saturated brine at the same bottomhole injection pressure.

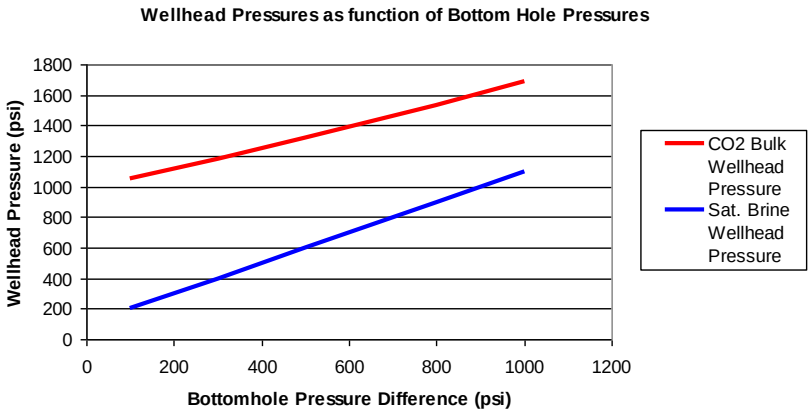

Figure 5—The wellhead pressure required to inject CO_2 (the red curve) is much higher (500 psi to 900 psi) than that required to inject brine (the blue curve) for the same bottomhole injection pressure. The rates of brine and of CO_2 are set at 35,000 B/D and 125 MMSCF/D respectively.

Assuming the injection wells are near where the mixing occurs, we assume the pressure at the wellhead will be equal to the mixing pressure for the saturated brine case.

Power Requirements

We modeled appropriate thermodynamic paths for the pressure-changing equipment. This permits us to determine the power required for each of the injection strategies of interest, CO_2-saturated brine and CO_2 bulk phase. The schematic for the compression of CO_2 process is shown in Figure 6.

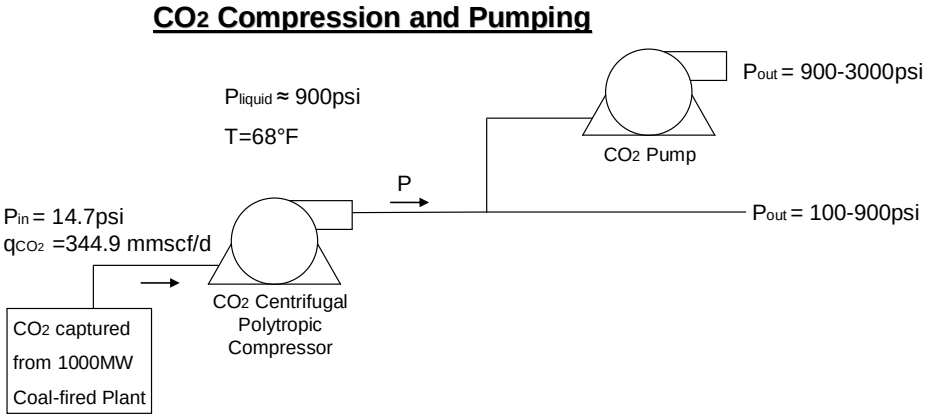

Figure 6—The compression of CO_2, in the less dense gas phase, is modeled as polytropic compression from 14.7psia to the liquid pressure at 900psia (equations and properties in Table 2 and 3). If a pressure above the liquid pressure is required, the additional pumping work is modeled as incompressible for a pressure-averaged density (see Table 2).

To estimate the work for compression of CO_2, we selected a multi-stage polytropic centrifugal compressor with ideal intercooling as discussed by Boyce (2005), using the parameters used in Fisher *et al.* (2005). As suggested by Fisher *et al.*, the multi-stage polytropic process is optimized to ensure the compression ratio never exceeds 3 and the outlet temperature never exceeds 350°F. After the phase change at around 900 psia, we modeled the pumping work (pumping implies liquid phase) as incompressible compression. We estimate the additional energy losses not associated with the compression and pumping of the fluid in an efficiency term (see Table 5). The necessary equations are found in Table 2 and come from Cengel & Boles (1989) and Boyce (2005). The properties and parameters for those equations were obtained from Cengel & Boles (1989) and Fisher *et al.* and are also found in Table 5. The power requirement for the compression of CO_2 increases with pressure as shown in Figure 8 and is consistent with other sources (Fisher, 2005; Ennis-King & Paterson, 2002).

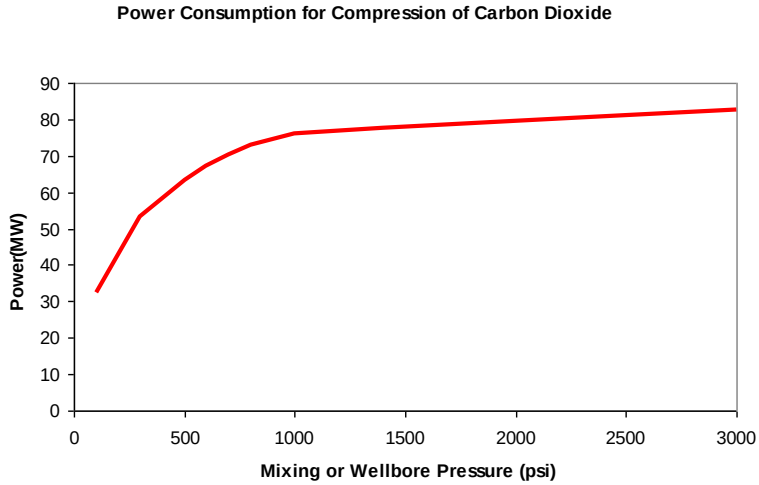

Figure 7— The power consumption for compression of CO_2 increases as shown for 344.9mmscf/d. The inlet pressure is 14.7 psi. As the discharge pressure increases, the fluid becomes more dense and the incremental power requirement decreases. Above pressures of 2000psia, 80MW (8% of the power output of the power plant) is consumed in compression which is consistent with other literature (Fisher, 2005; Ennis-King, 2002).

The process to pump 10,000ppm brine into the mixing tank is shown schematically in Figure 8. The brine is assumed incompressible, and—importantly—its flow rate is obtained from the solubility plots at the pressure of the mixing tank. The discharge pressure of the pump is the mixing tank pressure. The equations and parameters used to model brine pumping are found in Table 4 and Table 5. The power consumption for this compression as a function of mixing tank pressure is shown in Figure 9.

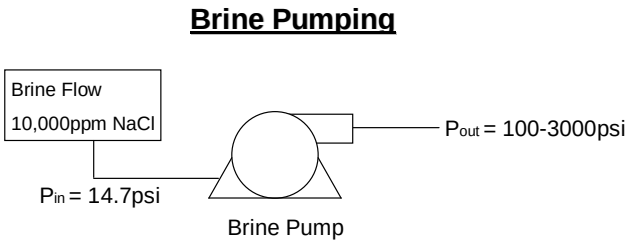

Figure 8—The power consumption for pumping 10,000 ppm NaCl brine to outlet or discharge pressure is modeled as incompressible compression.

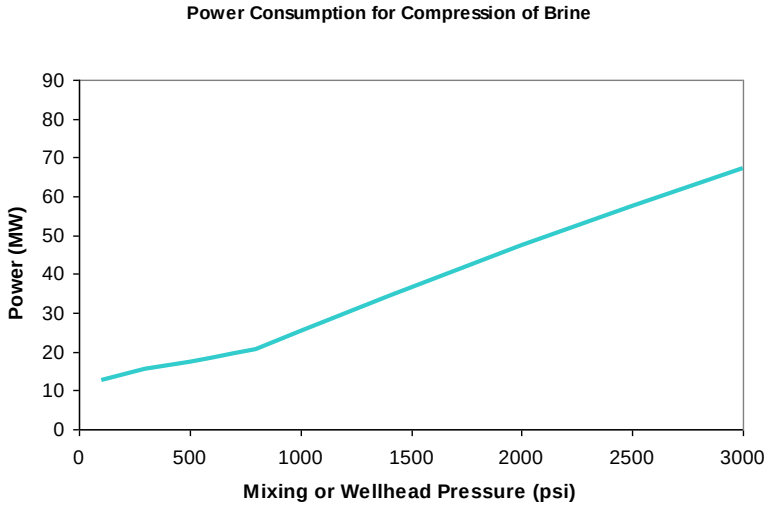

Figure 9—The power required for pumping the brine increases with pressure. Recall that the flow rate for the brine is based upon the Duan EOS model which is dependant on the mixing pressure (see Fig. 4).

In order to operate the mixing strategy, the brine and the carbon dioxide must be brought up to the same pressure for mixing, so the power requirement is the sum of the brine and CO_2 power curves (Fig. 7 and 9). From Figure 5, we recognize the mixing pressure (or wellhead pressure) will only range between 200 psia to 1100 psia for injection into the formation. In summary, Figure 10 is simply the sum of the brine and CO_2 consumption curve truncated over the range needed for injection.

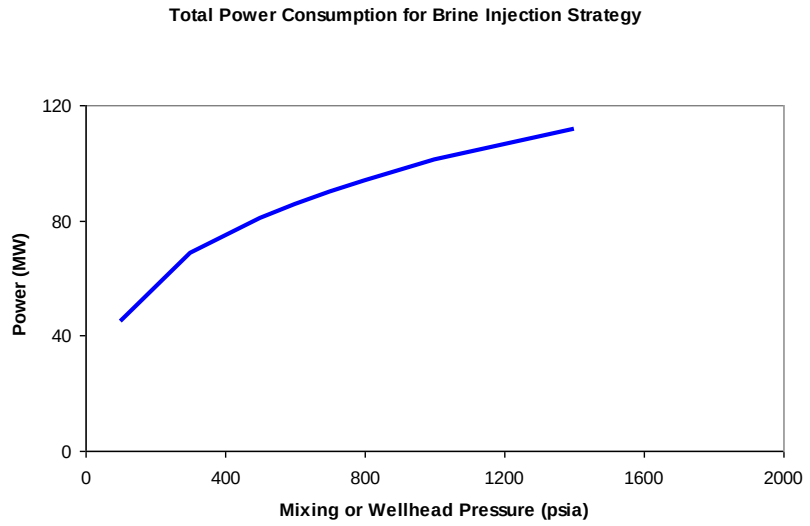

Figure 10—The total power consumption for the brine injection strategy is the addition of curves from Figures 8 and 9. The curve is truncated to show only the pressure range needed for injection into the aquifer. 50 MW to 110MW are needed to inject brine into the formation.

Similarly, the power requirement for the base case of CO_2 bulk phase injection is just the CO_2 power curve from Figure 7, with the compressor discharge pressure taken to be the wellhead pressure. In Figure 11, this power consumption curve is also truncated over the range of pressures needed for injection (1100 psia to 1700 psia, discharge or wellhead pressure).

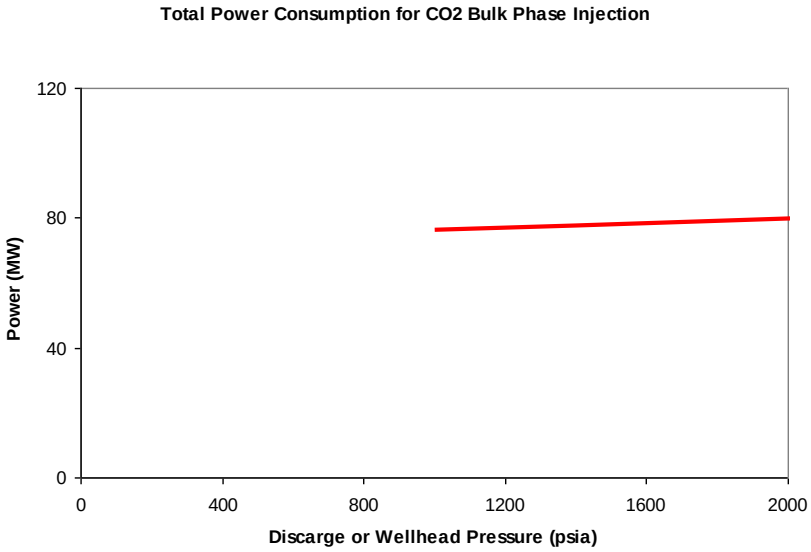

Figure 11—The estimated power consumption curve for the CO_2 bulk strategy varies only from 76 to 80 MW for the range of pressures needed to inject into the formation.

In summary, we estimate the power consumption for the brine injection strategy to be between 40 MW and 110 MW whereas the CO2 bulk phase injection estimation is 76 to 80 MW. The range of wellhead pressures needed is based upon the wellbore model in the previous section.

Capital Costs

The capital costs for each strategy are derived from estimated prices for the surface facilities and well construction.

For the saturated brine injection strategy, the capital costs included are the following: compressor purchase and setup, construction of injection wells, and a pressure vessel in which CO_2 dissolution occurs prior to brine injection. The compressor pricing was approximately $500,000 per MW of power consumed (Fisher, 2005). Injection wells were priced at $200,000 each, and are expected to handle 35,000bbl/d of saturated brine or 125 mmscf/d of CO_2. The cost of the pressure vessel for mixing depends upon the pressure, the flow rate, and the residence time for the CO_2 to dissolve. For a stainless steel vessel, the approximate cost will be $0.80 per pound manufactured and the equations used are found in Table 6. A residence time of one minute was assumed to be sufficient. The vessel dimensions and hence cost scale linearly with residence time so assessing this parameter is an important consideration. We are not aware of any processes from which a better estimate could be obtained. Figure 12 shows the estimated costs for compressors, injection wells, and the mixing pressure vessel as a function pressure for the saturated brine injection strategy. These curves are also truncated to the range of pressures needed at the wellhead for the brine injection strategy. (Remember only pressures between 200 psia to 1100 psia are needed at the wellhead for injection.)

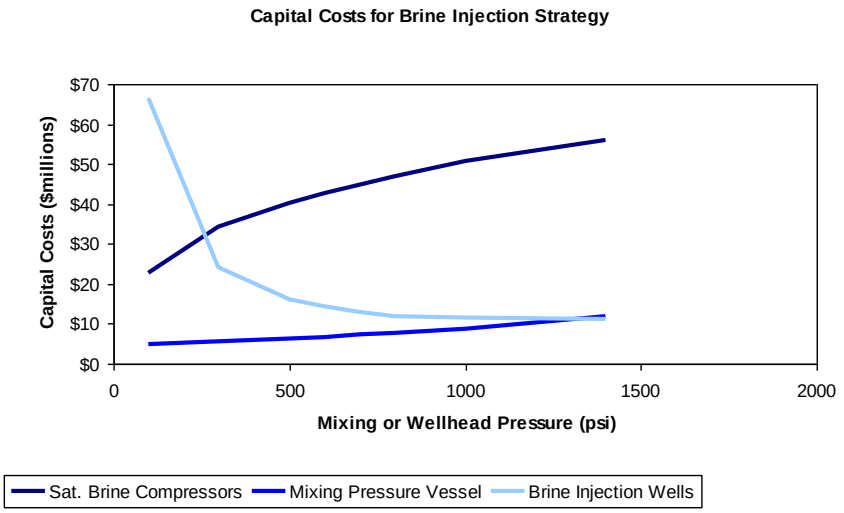

Figure 12—The capital costs of three necessary components for the saturated brine injection strategy (compressors, injection wells, and the mixing pressure vessel) vary with the wellhead pressure. The compressor curves (darkest blue) follow the power curves (Fig. 10). The mixing pressure vessel curve (blue) is a function of pressure, flow rate, and residence time (assumed to be one minute) for the CO_2 to dissolve. The injection well curve (light blue) follows the solubility curve (Fig. 4).

Similarly, the CO_2 bulk phase injection strategy will require compressors and injection wells. The prices for these are the same as in the previous strategy: $500,000 per MW of power consumed for compressor pricing, and $200,000 per injection well assuming each well can handle 125 mmscf/d of CO_2 (see Figure 13).

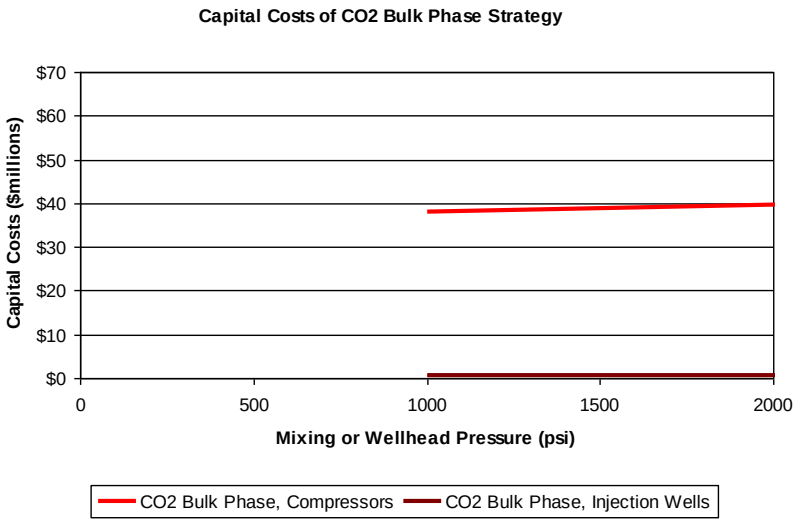

Figure 13— Capital costs of CO_2 bulk phase injection strategy include injection wells and compressors as a function of wellhead pressure. The compressor curve (red curve) follows the power curve for CO_2 compression (Fig. 6 and 9). Only three injection wells are needed for CO2 bulk phase injection (brown curve).

The total capital cost for the saturated brine injection strategy, as represented, is the sum of the compressors, injection wells, and mixing tank cost curves in Fig. 12. Similarly, the total capital cost for the CO_2 bulk phase curves in Fig. 13. Figure 14 contains these curves.

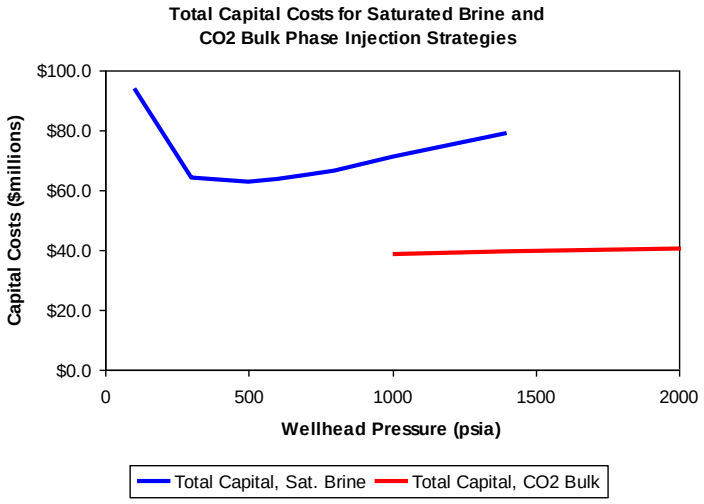

Figure 14— The capital costs for the saturated brine strategy (blue) and CO2 bulk phase strategy (red) are the sum of their representative curves (see Fig. 11 and 12). The CO_2 curve follows the power consumption curve. At mixing tank pressures (which equals wellhead pressures) below 300 psia, the brine curve is dominated by the cost of injection wells. Above 800 psia, the brine curve is dominated by the cost of compressors.

For the brine strategy, the capital costs of about $60 million are at an optimum between 300 psia and 700 psia. The bulk phase injection is about $40 million over the range of needed wellhead pressure.

Discussion

Having modeled the solubility, the power consumption, and the trends in capital costs, we can observe the trends, advantages, and disadvantages of each strategy. First, we will discuss each of the models and their sources of error and uncertainty.

From the solubility model, we demonstrate a tradeoff between mixing tank pressure and brine flow rate. At higher pressures (>800psia) a smaller flow rate of brine required (<3mmbbl/d). We assume that the dissolution goes to completion in the pressure vessel, but it is not known how long this will take (residence time) nor whether special efforts (internal baffles, stirrers, etc) are needed to bring the two phases into contact. The uncertainty of the Duan equation of state in the solubility curve will lead to a ±3% power consumption error. An error in salinity by ±10,000ppm will also lead to a ±3% error in power consumption. Solubility is known to be sensitive to the temperature, but we have not yet quantified the effect on power consumption. The total error from the solubility model, based on errors in salinity and the equation of state, is estimated at ±6% error in the power consumption of the saturated brine strategy.

In the wellbore model, a sensitivity study of the relative roughness, pipe diameter, and flow rate showed no important effects on the well bore model. The temperature profile in the CO_2 bulk phase injection could contribute to important error on the order of ±40%. Our assumption of isothermal flow in the well at both surface temperature (68°F) and reservoir temperature (141°F) provides an lower bound (-20%) and upper bound (+40%) on the wellhead pressure. Yet, the assumption of a linear temperature profile, in our judgment, is the most representative of our expectations in the well.

The power consumption model is sensitive to the efficiencies for the compression process. The assumed efficiencies should be verified by a manufacturer. An error in the estimated work for compression of CO_2 will affect both the saturated brine strategy and the CO_2 bulk phase strategy. Thus such an error changes the total cost of each process but does not change the difference in costs between the strategies. An error in the compression of brine can come from the solubility model previously discussed (resulting in a ±6% error in the power consumption of the saturated brine strategy) or an error in the compression efficiency (for example, ±10% will result in ±6% in the saturated brine compression power) for a total of ±12%.

The uncertainty associated with the capital costs is greater than for the operating costs. The capital costs are intended to demonstrate trends and did not include additional costs which could be important such as water treatment, brine transportation, or monitoring of CO_2 movement. We expect the transportation of the brine from its source and to the 50+ operating injection wells and the treatment of the brine could be important for some locations. The cost of the mixing tank is proportional to the residence time required, and there is very little information to constrain the residence time. The mixing tank accounts for 10-12% of the total capital cost. For the CO_2 injection strategy, monitoring equipment and risks associated with the CO_2 migration are not included.

Although the comparison can clearly be made between the two strategies (Fig. 10, 11, and 14), we plotted by means of the transformation alluded to in the wellbore model section. Since the bottomhole pressure difference was constrained between 100 psi and 1000 psi, we use this scale to “slide” the curves on top of one another. The bottomhole pressure difference is a transform of the dependant variable (mixing/wellhead pressure)

through Figure 5. Figure 15 shows the power curves in terms of the bottomhole pressure; this figure just condenses Figure 10 and 11.

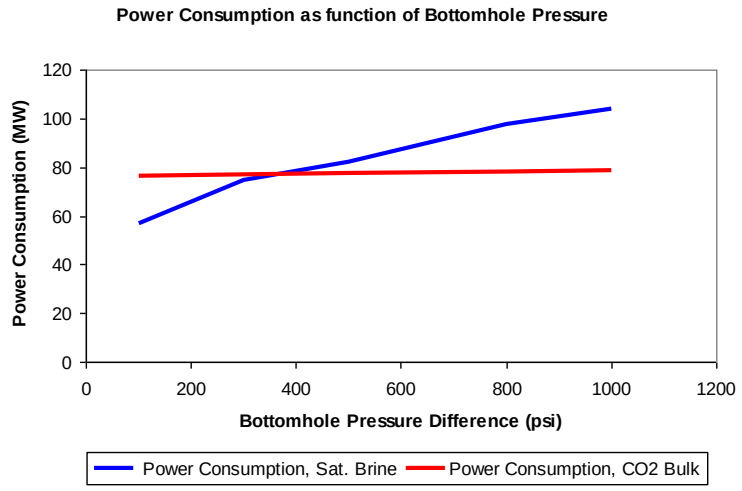

Figure 15—Combining the information from Fig. 5, 10, and 11, we show that the power consumption for the brine injection strategy (blue) can be less than for CO_2 injection. The CO_2 power consumption (red) changes very little over the range of possible injection pressures. We suggest from this curve that brine injection strategy would be competitive with CO_2 when the bottomhole pressure difference is less than 400psi which corresponds to mixing (or wellhead) pressures of 500psi or less.

We make the same transformation of the dependant variable (mixing/wellhead pressure) to view the curves. We combine Figure 5 and Figure 14 to produce Figure 15 which is a more compact way of viewing the data. The difference in the capital costs is $20 to $60 million more for the brine strategy than for the CO_2 strategy. The brine curve is high at lower pressure due to the large volume of brine and associated the injection wells. The curve increases at higher pressures because of mixing pressure vessel and compressor costs.

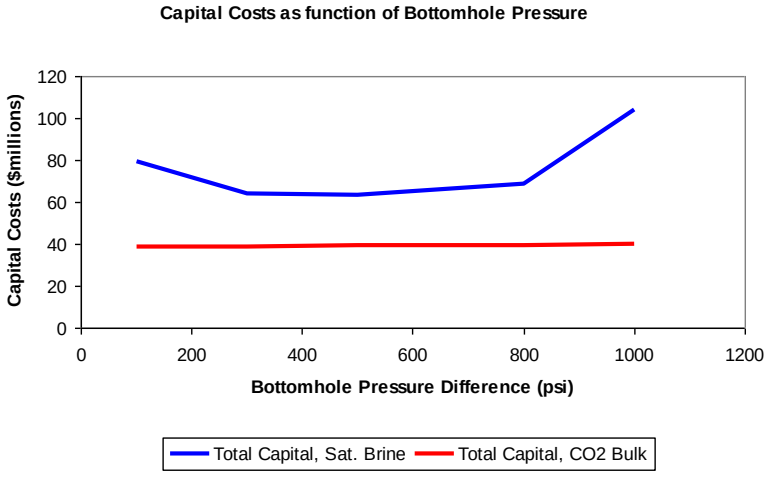

Figure 16—Transforming the information from Figure 14 by means of Figure 5, we estimate that the total capital costs for the saturated brine injection strategy (blue) is $20 to $60 million more than for the CO_2 bulk phase injection strategy (red). Compared with the $500 million investment needed for CO_2 capture, the capital costs summarized here are an important but small addition of capital. In the implementation of the saturated brine strategy, we would expect to pay ~4% more for additional initial capital but minimize the risk of leakage and avoid monitoring.

The additional capital cost ($20 million or 4% more), although important, should be compared with the capital costs expected for the CO_2 capture costs, the annual operation costs, and the long-term monitoring costs. From Fisher *et al.* (2005), the annual costs for an operation of an MEA stripping process will be approximately $500 million. The annual operational costs will be over $350 million per year at a price of $50 per tonne CO_2. Benson (2006) suggests monitoring costs will be on the order or $0.10 to $0.30 per tonne of CO_2 sequestered. For an injection period of 50 years, monitoring costs would be on the order of $36-$108 million. The most important advantage of a brine injection strategy is that the dissolution has already occurred, and saturated brine is secured.

Conclusion

The first and most important conclusion of the brine strategy is that no monitoring of the subsurface CO_2 will be necessary and risk of migration to the surface will be minimized.

Second, we estimate that the power consumption for injecting CO_2 saturated brine is comparable to that for injecting bulk phase CO_2 (see Fig. 14). Injecting saturated brine requires greater initial capital investment than required for injecting bulk CO_2 (see Fig. 15) and a large volume of available brine. Sources such as seawater, waste water, or fresh water could be used as brine.

Finally, we have also calculated important capital costs associated with the two strategies including compressors, injection wells, and mixing pressure vessels. We conclude that the capital costs for the brine strategy will exceed those of the bulk phase CO_2 by 50% to 100%, but represent a small fraction (~4-12%) of the capital and a smaller fraction (~6%) of the annual operating budget of the capture and sequester venture.

Recommendations for further work include estimating additional capital costs for both strategies including brine transportation costs (pipelines), reservoir characterization (depth, pressure, and temperature), monitoring costs (wells and groundwater monitoring), surface facilities (mixing of brine and CO_2), brine source and treatment (ocean, river, waste, or aquifer), and risk assessment (faults, seal, and wells and associated costing consequences). Many of the recommendations will require site specific information to accurately quantify them.

Of the future work, for most will be to determine if such substantial amount of brine can be obtained and what the true costs would be. The injection of 3 mmbbl/d would result in a sizeable footprint. One square mile of brine in a 1000ft formation would be displaced each year of injection.

Acknowledgements

We are grateful to the sponsors of the Geologic CO_2 Storage Joint Industry Project at UT-Austin: Chevron, CMG, ENI, ExxonMobil, Shell and TXU.

References

Benson S. M., (2006) Monitoring Carbon Dioxide Sequestration in Deep Geological Formation for Inventory Verification and Carbon Credits. SPE 102833. Proceeding of SPE: Annual Technical Conference and Exhibition

Boyce, Meherwan P., (2005) Centrifugal Compressors: A Basic Guide, Tulsa, OK: PennWell

Cengel Y. and Boles M., (1989) Thermodynamics: An Engineering Approach. New York: McGraw Hill

Economides, M., Hill, A., and Ehlig-Economides, C. (1993) Petroleum Production Systems. Upper Saddle, New Jersey: Prentice Hall

Ennis-King, J. and Paterson, L. (2002). Engineering Aspects of Geological Sequestration of Carbon Dioxide. SPE 77809. Presented at the Asia Pacific Oil and Gas Conference and Exhibition.

Fisher, K., Beitler, C., Rueter, C., Searcy, K., Rochelle, G., Jassim, M., (2005) Integrating MEA Regeneration with CO_2 Compression and Peaking to Reduce CO_2 Capture Costs. DOE Final Report Work Performed Under Grant No.: DE-G02-04ER84111

Hangx, S. (2005) Behavior of the CO2-H2O system and preliminary mineralisation model and experiments. CATO Workpackage WP 4.1, Deliverable WP 4.1-3-05 p. 1-43.

Weibe, R., and Gaddy, L., (1940) The Solubility of Carbon Dioxide in Water at Various Temperatures from 12 to 40° and at Pressures to 500 Atmospheres: critical phenomena, J. Am. Chem. Soc62, 815-817.

Table 1—Carbon dioxide disposal rates for 1000MW coal-fired power plant are shown after 90% capture.		
Captured Yearly Mass Flow Rate	7,200,000	tonne/year
Captured Daily Mole Rate ($\dot{N}$)	988,000	lbmol/day
Captured Volumetric Flow Rate (q_{CO2})	344.9	mmscf/day
Captured Daily Mass Flow Rate ($\dot{m}_{tonne}$)	19,700	tonne/day

Table 2—The bottomhole pressure difference can be estimated from the steady-state reservoir performance equation given in Economides *et al.* (1993).	
Steady-State Reservoir Performance	$\Delta p = \frac{141.2 q B \mu}{kh} \ln \frac{r_e}{r_w} (psi)$
Radius of edge, r_e	10^4 ft
Saturated Brine Strategy Flow rate, Volume factor and Viscosity product, $qB\mu_{brine}$	17,500 bbl-cp/d

CO_2 Bulk Phase Strategy Flow rate, Volume factor, and Viscosity product, $qB\mu_{CO2}$	4,350 bbl-cp/d
Saturated Brine Strategy Permeability Height Product, kh	Varied from $2.5x10^4$-$2.5x10^5$ (md-ft)
CO_2 Bulk Phase Strategy Permeability Height Product, kh (which is ¼ of the kh for brine)	Varied from $6.4x10^3$-$6.4x10^4$ (md-ft)

Table 3—The mechanical energy balance can be discretized using forward difference approximation. The general equations were obtained from Economides *et al.* and the properties from PVTsim.

Mechanical Energy Equation	$P_{n+1}=P_n+\rho g\Delta L+\frac{2\rho f_f u^2\Delta L}{D}$
Mean Velocity, u	$u=\frac{4q_{sc}\rho_{sc}}{\pi D^2\rho}$
Density, ρ (Linear interpolation of PVTsim data at 68°F and 141°F)	$\rho_{CO_2}=\rho\left(P_{n+1}+P_n/2, T\right),\ \rho_{brine}=62.4\,lb/ft^3$
Viscosity, μ (Linear interpolation of PVTsim data at 68°F and 141°F)	$\mu_{CO_2}=\rho\left(P_{n+1}+P_n/2, T\right),\ \mu_{brine}=1.0cp$
Temperature, T	Linear Temperature Profile (68°F at surface, 141°F at res.)
Friction Factor, f_f	Colebrook-White Equation
Relative Roughness, ε	0.0006
Diameter of Wellbore, D	4” for CO_2 and 10” for Saturated Brine

Table 4—The compression equations for CO2 and brine compression were modeled according following the equations of Cengel & Boles (1989) and Boyce (2005). These equations do not show the unit conversions. Symbols in the equations are defined in Tables 1 and 3.

Volumetric Brine Flow Rate	$q_{brine} = \frac{M_{W,brine}\dot{N}\left(1/m_f - 1\right)}{\rho_{Brine}}$
Volumetric Flow rate of liquid CO_2	$q_{liquid} = \frac{NM_{w,CO_2}}{\rho_{avg,CO_2}}$
Multi-Stage Polytropic Compression (where S is number of stages)	$W = \frac{SNnRT_1}{n-1}\left(\left(\frac{P_x}{P_1}\right)^{n-1/n} - 1\right)$
Compression of Incompressible Fluid	$W = q_{liquid}(P_{final} - P_{liquid})$
Pump or Process Efficiency (η) (for isothermal, isentropic, and polytropic processes)	$W_{input} = \frac{W_{process}}{\eta}$
k (obtained from solution of)	$\Delta h = \frac{kRT_1}{k-1}\left(\left(\frac{P_x}{P_1}\right)^{k-1/k} - 1\right)$
Intermediate Pressure	$P_x = P_1\left(P_{liquid}/P_1\right)^{\frac{1}{S}}$
Polytropic Coefficient (n) and Polytropic Efficiency η_p	$n = \frac{k\eta_p}{1+k\eta_p - k}$
Outlet Temperature	$T_{final} = T_1\left(\frac{P_{final}}{P_1}\right)^{k-1/k}$

Table 5—The thermodynamic properties and process efficiencies for CO2 and brine compression were modeled according following the parameters of Cengel & Boles (1989) and Fisher *et al.* (2005).	
R (gas constant)	$1.968 \frac{\text{BTU}}{\text{lbmole} \cdot \text{R}^\circ}$
Enthalpy	$\Delta h = [5.316 + 7.9361\text{E-}3 \left(\frac{T_2 + T_1}{2} \right) - 2.581\text{e-}6 \left(\frac{T_2 + T_1}{2} \right)^2 + 3.059\text{E-}10 \left(\frac{T_2 + T_1}{2} \right)^3](T_2 - T_1)$ BTU/lbmol
T_1 (assumed)	68°F or 528°R
P_1,P_{final} (assumed)	14.7psia, 100-3000psia
k (ratio of specific heats)	1.284 to 1.276
n (polytropic coefficient)	1.385 to 1.373
η_p (polytropic efficiency)	79.6%
$\eta_{compressor,CO_2}$ (assumed)	80%
$\eta_{pump,brine}$ (assumed)	80%
η_{pump,CO_2}	60%
S (number of stages)	4
P_{liquid} at 68F for CO_2	900psia
ρ_{avg,CO_2} (average of value at P_{liquid} and P_{final})	43.3-49.7 lb/ft^3
ρ_{brine}	62.4 lb/ft^3
Molecular Mass ($M_{W,CO2}$)	44.01 lb/lbmol
Molar Mass ($M_{W,brine}$)	18.01 lb/lbmol

Table 6—The mixing pressure vessel is sized by the pressure, flow rate, and residence time.	
Hoop Stress	$\sigma = \frac{prFS}{t}$
Volume of Vessel	$V_{tank} = \pi r^2 L = (q_{brine} + q_{co2})t_r$
Volume of Stainless Steel	$V_{steel} = 2\pi rtL$
Price of Vessel	$\$_{steel} \rho_{steel} V_{steel}$
Factor of Safety, FS	3.0
Residence Time, t_r	1.0 minute